



1 Addressing the assumption of stationarity in statistical bias  
2 correction of temperature.

3 **Manolis G. Grillakis<sup>1</sup>, Aristeidis G. Koutroulis<sup>1</sup>, Ioannis N. Daliakopoulos<sup>1</sup>, and**  
4 **Ioannis K. Tsanis<sup>1,2</sup>**

5  
6 [1] {Technical University of Crete, School of Environmental Engineering, Chania, Greece}

7 [2] {McMaster University, Department of Civil Engineering, Hamilton, ON, Canada}

8

9 Manolis G. Grillakis Ph.D.

10 Phone: +30.28210.37728, Fax: +30.28210.37855, e-mail: [manolis@hydromech.gr](mailto:manolis@hydromech.gr)

11

12 Aristeidis G. Koutroulis Ph.D.

13 Phone: +30.28210.37764, Fax: +30.28210.37855, e-mail: [aris@hydromech.gr](mailto:aris@hydromech.gr)

14

15 Ioannis N. Daliakopoulos Ph.D.

16 Phone: +30.28210.37800, Fax: +30.28210.37855, e-mail: [daliakopoulos@hydromech.gr](mailto:daliakopoulos@hydromech.gr)

17

18 Ioannis K. Tsanis Ph.D.

19 Phone: +30.28210.37799, Fax: +30.28210.37849, e-mail: [tsanis@hydromech.gr](mailto:tsanis@hydromech.gr)

20

21

22

23 **correspondence email for proofs: [manolis@hydromech.gr](mailto:manolis@hydromech.gr)**



24

25 **Abstract**

26 Bias correction of climate variables has become a standard practice in Climate Change  
27 Impact (CCI) studies. While various methodologies have been developed, their majority  
28 assumes that the statistical characteristics of the biases between the modeled data and  
29 the observations remain unchanged in time. However, it is well known that this  
30 assumption of stationarity cannot stand in the context of a climate. Here, a method to  
31 overcome the assumption of stationarity and its drawbacks is presented. The method is  
32 presented as a pre-post processing procedure that can potentially be applied with  
33 different bias correction methods. The methodology separates the stationary and the non-  
34 stationary components of a time series, in order to adjust the biases only for the former  
35 and preserve intact the signal of the later. The results show that the adoption of this  
36 method prevents the distortion and allows for the preservation of the originally modeled  
37 long-term signal in the mean, the standard deviation, but also the higher and lower  
38 percentiles of the climate variable. Daily temperature time series obtained from five Euro  
39 CORDEX RCM models are used to illustrate the improvements of this method.

40

41

42

43

44

45

46

47

48

49 **Keywords:** temperature non-stationarity, trend preservation, statistical bias correction,



## 50 **1 Introduction**

51 Climate model output consist the primary source of information used to quantify the effect  
52 of the foreseen anthropogenic climate change on natural systems. One of the most  
53 common and technically sound practices in Climate Change Impact (CCI) studies is to  
54 calibrate impact models using the most suitable observational data and then to replace  
55 observational data with the climate model data in order to assess the effect of potential  
56 changes in the climate regime. Often, raw climate model data cannot be used in CCI  
57 models due to the presence of biases in the representation of regional climate  
58 (Christensen et al., 2008; Haerter et al., 2011). In fact, hydrological CCI studies outcomes  
59 have been reported to become unrealistic without a prior adjustment of climate forcing  
60 biases (Hansen et al., 2006; Harding et al., 2014; Sharma et al., 2007). These biases may  
61 be attributed to a number of sources such as the imperfect representation of the physical  
62 processes within the model code and the coarse spatial resolution of output that do not  
63 permit the accurate representation of small-scale processes. Furthermore, climate model  
64 tuning for global projections focuses on essential elements such as the adequate  
65 representation of feedbacks between processes and hence the realistic depiction of a  
66 variable, such as temperature, against observations can be sidelined (Hawkins et al.,  
67 2016).

68 A number of statistical bias correction methods have been developed and successfully  
69 applied in CCI studies (e.g. Grillakis et al., 2013; Haerter et al., 2011; Ines and Hansen,  
70 2006; Teutschbein and Seibert, 2012). Their main task is to adjust the statistical  
71 properties of climate simulations to resemble those of observations, in a common  
72 climatological period. This is typically accomplished with the use of a Transfer Function  
73 (TF) which minimizes the difference between the cumulative distribution function (CDF)  
74 of the climate model output and that of the observations, a process also referred to as  
75 quantile mapping. As a result of quantile mapping, the reference (calibration) period's  
76 adjusted data are statistically closer, and sometimes near-identical to the observations.  
77 Thus the statistical outcomes of an impact model run using observational data are likely  
78 to be reproduced by the adjusted data. The good performance of statistical bias correction  
79 methods in the reference period is well documented (Grillakis et al., 2013; Ines and



80 Hansen, 2006; Olsson et al., 2015). Under the assumption of climate stationarity, the TF  
81 is then applied to data beyond the time-frame of the observations.

82 A process is characterized as stationary when the probability distribution function (PDF)  
83 of its state fluctuates within an unchanging and time invariant interval, or in a looser  
84 definition, when the process retains its mean, variance and auto covariance structure  
85 constant (Challis and Kitney, 1990). Ergo is the definition of stationary “bias” which refers  
86 to the time independent component of the difference between the modeled and the  
87 observed values (Haerter et al., 2011). Stationarity has been observed in long  
88 observational hydrological time series (Koutsoyiannis, 2002; Koutsoyiannis and  
89 Montanari, 2015; Lins and Cohn, 2011; Matalas, 2012). Nevertheless, non-stationarity is  
90 “unequivocal and unconditional” to all natural systems (Lins and Cohn, 2011), hence  
91 considering long-term climate or other processes involving abrupt system changes as  
92 stationary is certainly flawed. Therefore, the stationarity-dependent extrapolation of the  
93 TF is often regarded as a leap of faith and may lead to a false certainty about the  
94 robustness of the adjusted projection.

95 As the most obvious effect, the assumption of stationarity in bias correction adds another  
96 level of uncertainty in the output (Maraun, 2012). At a more practical level, it may also  
97 lead to other unwanted effects, such as changes in the original model derived long-term  
98 trend or other higher moments of the climate variable statistics that eventually distort the  
99 long-term signal of the climate variable. As an example, Olsson et al. (2015) showed that  
100 their distribution based scaling (DBS) bias correction methodology might alter the long-  
101 term temperature trends. They attribute the phenomenon in the severity of the biases in  
102 the mean or the standard deviation between the uncorrected temperatures and the  
103 observations. Similar conclusions were drawn by Hagemann et al. (2011) who showed  
104 that a fixed bias correction can alter the climate change signal for specific locations and  
105 seasons and concluded that climate parameters require variable adjustment as the  
106 distribution between their upper and lower limit changes in time. In their work, Hempel et  
107 al. (2013) attempt to provide a solution to the trend changing issue, by preserving the  
108 absolute changes in monthly temperature, and relative changes in monthly values of  
109 precipitation. The obvious conceptual drawback of this approach is that non-stationarity  
110 does not always coincide with a deterministic trend component (Lins, 2012).



111 While climate may be considered stationary for the studied time scales (i.e. a few  
112 decades), it is uncertain whether this stationarity holds between intervals selected for bias  
113 correction. Narrow time windows may obscure information about a recurring periodicity  
114 thus attributing non-stationarity to the data. Instead, in a time window sufficiently larger  
115 than underlying periodicities, the same signal may reveal to be part of a stationary  
116 process. A representative example about the role of timescales in non-stationarity is  
117 illustrated by Koutsoyiannis and Montanari (2015). In the context of climate change, the  
118 concept of climate non-stationarity is discussed beyond the profound daily and seasonal  
119 periodicities. Milly et al., (2008) denote as stationary a climate process response with  
120 time-invariant probability distribution in one year periodic. This is a reasonable  
121 assumption in the context of CCI studies, as seasonal is the most well defined periodicity  
122 of a climate system at least in the time scale of a few decades. Reversely, when the year-  
123 to-year distribution of a climate process response changes, the variable can be described  
124 as non-stationary, thus leading to the unwanted effects of quantile mapping based bias  
125 correction methods described in Olsson et al. (2015). As the TF of the bias correction is  
126 estimated between the reference period observations and climate model data, it indicates  
127 the different magnitude of correction for the different parts of the probability distribution  
128 function (PDF). Considering that the climate data PDF is actually time-dependent (i.e. non  
129 stationary), the stationary TF gradually changes its response on the climate data,  
130 providing unequal bias correction in different periods as Hagemann et al. (2011) also  
131 notice.

132 Figure 1 presents an indicative example where temperature data<sup>1</sup> have a mean bias of  
133 2.02 °C in the reference period (Figure 1a). The average bias is expressed by the average  
134 horizontal distance between the TF and the bisector of the central plot. The histogram on  
135 the left illustrates the reference period modeled data for 1981-2010. The histogram at the  
136 bottom is derived from observational data. The histogram on the right is derived from a  
137 moving 30-year period between 1981 and 2098. In the rightmost histogram, the difference  
138 between the reference period and the moving 30-year period is estimated. The red mark

---

<sup>1</sup> The Figure 1 data were obtained from ICHEC-EC-EARTH r12i1p1 SMHI-RCA4\_v1 Euro-CORDEX simulation under the RCP85, for the location Chania International Airport (lon=24.08 lat=35.54).



139 shows the theoretical change in the average correction applied by the TF, due to the  
140 changes in the projected temperature histogram. Hence, the average correction applied  
141 for the 2068-2097 period reaches 3.48 °C, significantly higher than the reference period's  
142 bias (Figure 1b). The time-dependency of the correction magnitude introduces a long term  
143 signal distortion in the corrected data. In the quantile mapping based correction  
144 methodologies where the TF distance from the bisector is variable, this side effect is  
145 unavoidable. Nevertheless, in cases where the TF retains a relatively constant distance  
146 to the bisector (i.e. parallel to the bisector), the trend of the corrected data remains similar  
147 to the raw model data regardless of the temporal change in the model data histogram.

148 In this study, we present a methodology to account for the non-stationarity of the climate  
149 parameters. The methodology takes the form of a pre- and post-processing module that  
150 can be applied along with different statistical bias correction methodologies. To account  
151 for the non-stationarities, the method separates the stationary from the non-stationary  
152 components of a time series before it is bias adjusted. Bias correction is then applied to  
153 the stationary-only components of the time series. Finally, the non-stationary components  
154 are again merged to the adjusted component to form a single corrected time series. In  
155 order to use and test the module, we employ a generalized version of the Multi-segment  
156 Statistical Bias Correction (MSBC) methodology (Grillakis et al., 2013) that can be used  
157 in a wider set of climate parameters.

158

## 159 **2 Methods**

### 160 **2.1 Terminology**

161 As non-stationary components are identified the statistical deviations of each year's data  
162 comparing to the average reference period data distribution. Specifically, the differences  
163 between the CDF of each year's model climate data comparing to the CDF of the entire  
164 reference period of the model data are identified as the non-stationary component.  
165 Hence, the first step of the procedure is to normalize each year's data individually, against  
166 the average modeled reference period climatology. Let  $S_R$  be the reference period model  
167 data and  $S_i$  the climate data for year  $i$ , then the normalized data  $S_i^n$  for year  $i$  are



168 estimated by transferring each year data onto the average reference period CDF through  
169 a transfer function  $TF_{S_i}$  estimated annually. This can be formulated as Eq. 1.

$$S_i^n = TF_{S_R}^{-1} \left( TF_{S_i} (S_i) \right) \quad \text{Eq. (1)}$$

170 The difference between the original model data  $S_i$  and the normalized data  $S_i^n$  is the non-  
171 stationary component  $S_i^{NS}$  of the time series (Eq. 2).

$$S_R^{NS} = S_R - S_R^n \quad \text{Eq. (2)}$$

172 The original model data  $S_i$  can be reconstructed by adding the non-stationary  
173 components  $S_i^{NS}$  to the normalized data  $S_i^n$  as in Eq. 3.

$$S_i = S_i^{NS} + S_i^n \quad \text{Eq. (3)}$$

174 The non-stationary components ( $S_i^{NS}$ ) contain the random part of the climate signal, as  
175 well as the potential long-term changes in the statistics. After the separation, the  
176 stationarized climate model data are statistically bias corrected following a suitable  
177 methodology. The stationarized components of the modeled data are bias adjusted  
178 disregarding the stationarity assumption, as the data to be corrected are stationary. The  
179 non-stationary components ( $S_i^{NS}$ ) are preserved in order later to be added again to the  
180 bias corrected time series. We refer to the described method as non-stationarity module  
181 (NSM) to hereafter lighten the nomenclature of the paper.

182

## 183 **2.2 Bias correction**

184 The NSM is applied along with a modification of the MSBC algorithm proposed by Grillakis  
185 et al. (2013). This methodology follows the principles of quantile mapping correction  
186 techniques and was originally designed and tested for GCM precipitation adjustment. The  
187 novelty of the method is the partitioning of the data CDF space into discrete segments  
188 and the individual quantile mapping correction in each segment, thus achieving better fit  
189 of the parametric equations on the data and better correction especially on the CDF  
190 edges. The optimal number of the segments is estimated by Schwarz Bayesian  
191 Information Criterion (SBIC) to balance between complexity and performance.



192 Here the methodology is modified to use linear functions instead of the gamma functions  
193 used in the original methodology. Moreover, the upper and lower edge segments are  
194 explicitly corrected using only the mean difference between the reference period of the  
195 model data and the observations. This choice costs to the methodology, the remainder of  
196 some bias in the corrected data. However, it provides robustness, avoiding unrealistic  
197 temperature values at the edges of the model CDF. The bias correction methodology  
198 modification has been already used in the Bias Correction Intercomparison Project (BCIP)  
199 (Nikulin et al., 2015), while produced adjusted data have been used in a number of CCI  
200 studies (Daliakopoulos et al., 2016; Grillakis et al., 2016; Koutroulis et al., 2016;  
201 Papadimitriou et al., 2016). As the MSBC methodology belongs to the parametric quantile  
202 mapping techniques, it shares their advantages and drawbacks. A comprehensive  
203 shakedown of advantages and disadvantages of quantile mapping in comparison to other  
204 methods can be found in Maraun et al. (2010) and Themeßl et al. (2011).

205

### 206 **3 Case study**

207 To examine the effect of NSM on the bias correction, the Hadley Center Central England  
208 Temperature (HadCET - Parker et al., 1992) observational dataset was considered to  
209 adjust the simulated output from the earth system model MIROC-ESM-CHEM<sup>2</sup> historical  
210 emissions run between 1850 and 2005 for Central England. The Klemes (1986) split  
211 sample test methodology was adopted here for verification. The methodology considers  
212 two periods of calibration and validation, between the observed and modeled data. The  
213 first period is used for the calibration, while the second period is used as a pseudo-future  
214 period in which the adjusted data are assessed against the observations. To resemble a  
215 typical CCI study, the available 50 years of data between 1850 and 1899 served as  
216 calibration period, while the rest of the data between 1900 and 2005 was used as pseudo-  
217 future period for the validation. The bias correction results of the two procedures, with  
218 (BC-NSM) and without (BC) the non-stationarity module, were then compared against the  
219 observations. Figure 2a demonstrates the division of the raw data performed by the NSM  
220 into non-stationary components and normalized raw data in annual aggregates. The  
221 summation of the two time series can reconstruct the initial raw data time series. The  
222 normalized time series do not exhibit any trend or significant fluctuation in the annual



223 aggregates, since the normalization is performed at annual basis, while the long-term  
224 trend and the variability is contained in the residual time series.

225 In Figure 2b, annual aggregates obtained via the above two procedures are compared to  
226 the raw data and the observations. Results show that both procedures adjust the raw data  
227 to better fit the observations in the calibration period 1850-1899. In the validation period,  
228 both procedures produce similar results, but the BC-NSM long-term linear trend is slightly  
229 lower than that of the BC results. While the latter slope is closer to the observations' linear  
230 trend, the former is closer to the raw data trend (Table 1). The persistence of the long-  
231 term trend is a desirable characteristic of the NSM procedure as the GCM long-term  
232 moments were not distorted by the correction. However, the wider deviation of the BC-  
233 NSM trend relatively to the BC depicts the skill of the GCM to simulate the observations'  
234 respective trend. Figure 2c shows that the BC-NSM output resemble the raw data  
235 histograms in shape, but are shifted in their mean towards the observations. This consists  
236 an idealized behavior for the adjusted data, as the distribution of the annual temperature  
237 averages are retained after the correction. Similar results generated on daily data (Figure  
238 2d) show that both procedures adjust the calibration and validation histograms in the  
239 same degree towards the observations. This can also be verified by the mean, the  
240 standard deviation and the 5<sup>th</sup> and 95<sup>th</sup> percentile of the daily data (Table 1). An early  
241 concluding remark about the NSM is that it improved the long-term statistics of the  
242 adjusted data towards the climate model signal, without sacrificing the daily scale quality  
243 of the correction.

244 The split sample test is also adopted to assess the efficiency of the procedures in a  
245 European scale application. Split sample is the most common type of test used for the  
246 validation of model efficiency. A drawback of the split sample test in bias correction  
247 validation operations is that the remaining bias of the validation period is a function of the  
248 bias correction methodology deficiency and the model deficiency itself to describe the  
249 validation period's climate, in aspects that are not intended to be bias corrected. That  
250 said, a skillful bias correction method should deal well in that context, as model  
251 "democracy" (Knutti, 2010), i.e. the assumption that all model projections are equally  
252 possible, is common in CCI studies with little attention to be given to the model selection.  
253 In order to scale up the split sample test, the k-fold cross validation test (Geisser, 1993)



254 is employed. In k-fold cross validation test, the data is partitioned into k equal sized folds.  
255 Of the k folds, one subsample is retained each time as the validation data for testing the  
256 model, and the remaining k-1 subsamples are used as calibration data. In a final test, the  
257 procedures are applied on a long-term transcend climate projection experiment to assess  
258 their effect in the long-term attributes of the temperature in a European scale application.

259

### 260 **3.1 Data**

261 Temperature data from the European division of Coordinated Regional Downscaling  
262 Experiment (CORDEX), openly available through the Earth System Grid Federation  
263 (ESGF), are used to evaluate the presented procedures. Data from five RCM models  
264 (Table 2) with 0.44° spatial resolution and daily time step between 1951-2100 are used.  
265 The projection data are considered under the Representative Concentration Pathway  
266 (RCP) 8.5, which projects an 8.5 W m<sup>-2</sup> average increase in the radiative forcing until  
267 2100. The European domain CORDEX simulations have been evaluated for their  
268 performance in previous studies (Kotlarski et al., 2014; Prein et al., 2015). Figure 3 shows  
269 the 1951-2005 daily temperature average and standard deviation for the five RCMs of  
270 Table 2. The RCMs' mean bias ranges between about -2 °C and 1 °C relatively to the  
271 EOBS dataset. The positive mean bias in all RCMs is mainly seen in Eastern Europe,  
272 while the same areas exhibit negative bias in standard deviation. Some of the bias is  
273 however attributed to the ability of the observational dataset to represent the true  
274 temperature. Discussion about the applicability of EOBS to compare temperature of  
275 RCMs control climate simulations can be found in Kyselý and Plavcová (2010). For the  
276 purposes of this work, the EOBS is assumed to accurately represent the past  
277 temperatures over Europe.

278 For the k-fold cross validation, the RCM data between 1951-2010 are split into 6 ten-year  
279 sections, comprising a 6-fold, 5 RCM ensemble experiment (Figure 4). Each section is  
280 validated once by using the rest five sections for the calibration. A total number of 30 tests  
281 are conducted using each procedure.



282 For the transient experiment, the RCM data between 1951 and 2100 are considered,  
283 using the 1951-2010 as calibration to correct the 1951-2100 data.

284

#### 285 **4 Results and discussion**

286 Figure 5 shows the mean surface temperature of the cross validation test. The mean of  
287 the raw temperature data and the observations are respectively equal for their calibration  
288 and the validation periods due to the design of the experiment. The correction results  
289 show that both bias corrections with and without the NSM, appropriately meet the needs  
290 of the correction. The differences between the calibration and validation averages with  
291 the corresponding observations show consistently low residuals. A significant difference  
292 between the two tests is that the NSM increases the residuals due to the exclusion of the  
293 non-stationary components from the correction process. Nonetheless, the scale of the  
294 residuals is considered below significance in the context of CCI studies, as it ranges only  
295 up to 0.035 °C. The increased residuals of the NSM are the trade off to the preservation  
296 of the model long-term climate change signal, in the transient experiment. Figure 6  
297 presents the long-term change in the signal of the mean temperature, for the 10<sup>th</sup> and 90<sup>th</sup>  
298 percentiles (in annual aggregates). The trends are estimated by a simple linear least  
299 square fit and are expressed in °C per century. The use of the NSM profoundly better  
300 preserved the long-term trend relatively to the raw model data in all three cases. Without  
301 using the NSM module, the distortion in the mean annual temperature trend lies between  
302 -0.5 and 0.5 degrees per century, while the distortion in the 10<sup>th</sup> and 90<sup>th</sup> percentiles are  
303 apparently more profound. Additionally, the northeastern Europe's 10<sup>th</sup> and 90<sup>th</sup>  
304 percentiles reveal a widening of the temperature distribution when NSM is not used. The  
305 widening is attributed to the considerable negative trend in the p10 and the considerable  
306 positive p90 trend in the same areas. The magnitude of the distortion is considerable and  
307 can potentially lead to CCI overestimation. In contrast, with the use of NSM the change  
308 in the trend is considerably reduced in most of the Europe's area.

309 The impact of NSM on the standard deviation is also significant. Figure 7 shows the  
310 evolution of the standard deviation for each model, in the cases of raw data and the bias  
311 corrected data using the BC and the BC<sub>NSM</sub>. The standard deviation is estimated for each



312 grid point and calendar year, and is averaged across the study domain. Results show that  
313 standard deviations of the adjusted data differ from the respective standard deviations of  
314 the raw data, in both adjustment approaches. This is an expected outcome, as raw model  
315 data standard deviations differ from the respective observed data standard deviation  
316 (Figure 7 d, e). However, the standard deviation differences between  $BC_{NSM}$  and the raw  
317 data (Figure 7 f) is significantly more stable than that the respective differences from BC  
318 (Figure 7 g), meaning that the signal of standard deviation is better preserved and does  
319 not inflate with time in the former case. Additionally, the variation of the standard  
320 deviations time series exhibits lower fluctuations.

321

## 322 **5 Conclusions**

323 This study elaborates on two correlated issues of statistical bias correction; the  
324 assumption of stationarity and the distortion of long-term trends. These challenges are  
325 addressed by a pre/post processing module (NSM) that can be applied along with  
326 statistical bias correction techniques. The results are validated from several points of  
327 view. First, it is shown that the use of the NSM module resulted in the long-term  
328 temperature trend preservation in the mean annual aggregates of the temperature, but  
329 also in the aggregates of the higher and lower percentiles. Furthermore, the examination  
330 of the standard deviation temporal evolution show that is better retained relatively to the  
331 raw data. The corrected variable retains some remaining biases in the control period,  
332 which however are low to significantly affect CCI study outcomes.

333 The main advantage of the proposed method compared to other trend preserving  
334 methods (e.g. Hempel et al., 2013), is that the preservation of the long-term mean trend  
335 is not the objective but rather an ineluctable consequence of excluding the non-  
336 stationarity components from the correction process. Nevertheless, it has to be stressed  
337 that a range of issues, such as the disruption of the physical consistency of climate  
338 variables, the mass/energy balance and the omission of correction feedback mechanisms  
339 to other climate variables (Ehret et al., 2012) have not been addressed. Beyond the  
340 benefits of statistical bias correction methods, these constrains remain unsurpassable  
341 challenges that can only be resolved within a climate model itself. Finally, one should



342 bare in mind that climate data quality prime driver is the climate model skillfulness itself.  
343 Statistical post processing methods like bias correction cannot add new information to the  
344 data but rather add usefulness to it, depending on the needs of each application.

345

## 346 **6 References**

347 Challis, R.E., Kitney, R.I., 1990. Biomedical signal processing (in four parts). *Med. Biol.*  
348 *Eng. Comput.* 28, 509–524. doi:10.1007/BF02442601

349 Christensen, J.H., Boberg, F., Christensen, O.B., Lucas-Picher, P., 2008. On the need  
350 for bias correction of regional climate change projections of temperature and  
351 precipitation. *Geophys. Res. Lett.* 35, L20709. doi:10.1029/2008GL035694

352 Daliakopoulos, I.N., Tsanis, I.K., Koutroulis, A.G., Kourgialas, N.N., Varouchakis, E.A.,  
353 Karatzas, G.P., Ritsema, C.J., 2016. The Threat of Soil Salinity: a European scale  
354 review. *CATENA*.

355 Ehret, U., Zehe, E., Wulfmeyer, V., Warrach-Sagi, K., Liebert, J., 2012. *HESS Opinions*  
356 “Should we apply bias correction to global and regional climate model data?” *Hydrol.*  
357 *Earth Syst. Sci.* 16, 3391–3404. doi:10.5194/hess-16-3391-2012

358 Geisser, S., 1993. *Predictive inference*. CRC press.

359 Grillakis, M.G., Koutroulis, A.G., Papadimitriou, L. V, Daliakopoulos, I.N., Tsanis, I.K.,  
360 2016. Climate-Induced Shifts in Global Soil Temperature Regimes. *Soil Sci.* 181,  
361 264–272.

362 Grillakis, M.G., Koutroulis, A.G., Tsanis, I.K., 2013. Multisegment statistical bias  
363 correction of daily GCM precipitation output. *J. Geophys. Res. Atmos.* 118, 3150–  
364 3162. doi:10.1002/jgrd.50323

365 Haerter, J.O., Hagemann, S., Moseley, C., Piani, C., 2011. Climate model bias correction  
366 and the role of timescales. *Hydrol. Earth Syst. Sci.* 15, 1065–1079. doi:10.5194/hess-  
367 15-1065-2011

368 Hagemann, S., Chen, C., Haerter, J.O., Heinke, J., Gerten, D., Piani, C., Hagemann, S.,  
369 Chen, C., Haerter, J.O., Heinke, J., Gerten, D., Piani, C., 2011. Impact of a Statistical



- 370 Bias Correction on the Projected Hydrological Changes Obtained from Three GCMs  
371 and Two Hydrology Models. <http://dx.doi.org/10.1175/2011JHM1336.1>.
- 372 Hansen, J.W., Challinor, A., Ines, A.V.M., Wheeler, T., Moron, V., 2006. Translating  
373 climate forecasts into agricultural terms: advances and challenges. *Clim. Res.* 33,  
374 27–41.
- 375 Harding, R.J., Weedon, G.P., van Lanen, H.A.J., Clark, D.B., 2014. The future for global  
376 water assessment. *J. Hydrol.* 518, 186–193. doi:10.1016/j.jhydrol.2014.05.014
- 377 Hawkins, E., Sutton, R., Hawkins, E., Sutton, R., 2016. Connecting Climate Model  
378 Projections of Global Temperature Change with the Real World. *Bull. Am. Meteorol.*  
379 *Soc.* 97, 963–980. doi:10.1175/BAMS-D-14-00154.1
- 380 Hempel, S., Frieler, K., Warszawski, L., Schewe, J., Piontek, F., 2013. A trend-preserving  
381 bias correction – the ISI-MIP approach. *Earth Syst. Dyn.* 4, 219–236.  
382 doi:10.5194/esd-4-219-2013
- 383 Ines, A.V.M., Hansen, J.W., 2006. Bias correction of daily GCM rainfall for crop simulation  
384 studies. *Agric. For. Meteorol.* 138, 44–53. doi:10.1016/j.agrformet.2006.03.009
- 385 Klemes, V., 1986. Operational testing of hydrological simulation models. *Hydrol. Sci. J.*  
386 31, 13–24. doi:10.1080/02626668609491024
- 387 Knutti, R., 2010. The end of model democracy? *Clim. Change* 102, 395–404.  
388 doi:10.1007/s10584-010-9800-2
- 389 Kotlarski, S., Keuler, K., Christensen, O.B., Colette, A., Déqué, M., Gobiet, A., Goergen,  
390 K., Jacob, D., Lüthi, D., van Meijgaard, E., Nikulin, G., Schär, C., Teichmann, C.,  
391 Vautard, R., Warrach-Sagi, K., Wulfmeyer, V., 2014. Regional climate modeling on  
392 European scales: a joint standard evaluation of the EURO-CORDEX RCM ensemble.  
393 *Geosci. Model Dev.* 7, 1297–1333. doi:10.5194/gmd-7-1297-2014
- 394 Koutroulis, A.G., Grillakis, M.G., Daliakopoulos, I.N., Tsanis, I.K., Jacob, D., 2016. Cross  
395 sectoral impacts on water availability at +2°C and +3°C for east Mediterranean island  
396 states: The case of Crete. *J. Hydrol.* 532, 16–28. doi:10.1016/j.jhydrol.2015.11.015
- 397 Koutsoyiannis, D., 2002. The Hurst phenomenon and fractional Gaussian noise made



- 398 easy. *Hydrol. Sci. J.* 47, 573–595. doi:10.1080/02626660209492961
- 399 Koutsoyiannis, D., Montanari, A., 2015. Negligent killing of scientific concepts: the  
400 stationarity case. *Hydrol. Sci. J.* 60, 1174–1183.  
401 doi:10.1080/02626667.2014.959959
- 402 Kyselý, J., Plavcová, E., 2010. A critical remark on the applicability of E-OBS European  
403 gridded temperature data set for validating control climate simulations. *J. Geophys.*  
404 *Res.* 115, D23118. doi:10.1029/2010JD014123
- 405 Lins, H.F., 2012. A Note on Stationarity and Nonstationarity. WMOCHy-AWG.
- 406 Lins, H.F., Cohn, T.A., 2011. Stationarity: Wanted Dead or Alive?1. *JAWRA J. Am. Water*  
407 *Resour. Assoc.* 47, 475–480. doi:10.1111/j.1752-1688.2011.00542.x
- 408 Maraun, D., 2012. Nonstationarities of regional climate model biases in European  
409 seasonal mean temperature and precipitation sums. *Geophys. Res. Lett.* 39, n/a-n/a.  
410 doi:10.1029/2012GL051210
- 411 Maraun, D., Wetterhall, F., Ireson, A.M., Chandler, R.E., Kendon, E.J., Widmann, M.,  
412 Brienen, S., Rust, H.W., Sauter, T., Themeßl, M., Venema, V.K.C., Chun, K.P.,  
413 Goodess, C.M., Jones, R.G., Onof, C., Vrac, M., Thiele-Eich, I., 2010. Precipitation  
414 downscaling under climate change: Recent developments to bridge the gap between  
415 dynamical models and the end user. *Rev. Geophys.* 48, RG3003.  
416 doi:10.1029/2009RG000314
- 417 Matalas, N.C., 2012. Comment on the Announced Death of Stationarity. *J. Water Resour.*  
418 *Plan. Manag.* 138, 311–312. doi:10.1061/(ASCE)WR.1943-5452.0000215
- 419 Milly, P.C.D., Betancourt, J., Falkenmark, M., Hirsch, R.M., Kundzewicz, Z.W.,  
420 Lettenmaier, D.P., Stouffer, R.J., 2008. Stationarity Is Dead: Whither Water  
421 Management? *Science* (80-. ). 319.
- 422 Nikulin, G., Bosshard, T., Yang, W., Bärring, L., Wilcke, R., Vrac, M., Vautard, R., Noel,  
423 T., Gutiérrez, J.M., Herrera, S., Others, 2015. Bias Correction Intercomparison  
424 Project (BCIP): an introduction and the first results, in: EGU General Assembly  
425 Conference Abstracts. p. 2250.



- 426 Olsson, T., Jakkila, J., Veijalainen, N., Backman, L., Kaurola, J., Vehviläinen, B., 2015.  
427 Impacts of climate change on temperature, precipitation and hydrology in Finland –  
428 studies using bias corrected Regional Climate Model data. *Hydrol. Earth Syst. Sci.*  
429 19, 3217–3238. doi:10.5194/hess-19-3217-2015
- 430 Papadimitriou, L. V, Koutroulis, A.G., Grillakis, M.G., Tsanis, I.K., 2016. High-end climate  
431 change impact on European runoff and low flows – exploring the effects of forcing  
432 biases. *Hydrol. Earth Syst. Sci.* 20, 1785–1808. doi:10.5194/hess-20-1785-2016
- 433 Parker, D.E., Legg, T.P., Folland, C.K., 1992. A new daily central England temperature  
434 series, 1772–1991. *Int. J. Climatol.* 12, 317–342. doi:10.1002/joc.3370120402
- 435 Prein, A.F., Gobiet, A., Truhetz, H., Keuler, K., Goergen, K., Teichmann, C., Fox Maule,  
436 C., van Meijgaard, E., Déqué, M., Nikulin, G., Vautard, R., Colette, A., Kjellström, E.,  
437 Jacob, D., 2015. Precipitation in the EURO-CORDEX  $0.11^{\circ}$  and  
438  $0.44^{\circ}$  simulations: high resolution, high benefits? *Clim. Dyn.* 46,  
439 383–412. doi:10.1007/s00382-015-2589-y
- 440 Sharma, D., Das Gupta, A., Babel, M.S., 2007. Spatial disaggregation of bias-corrected  
441 GCM precipitation for improved hydrologic simulation: Ping River Basin, Thailand.  
442 *Hydrol. Earth Syst. Sci.* 11, 1373–1390. doi:10.5194/hess-11-1373-2007
- 443 Teutschbein, C., Seibert, J., 2012. Bias correction of regional climate model simulations  
444 for hydrological climate-change impact studies: Review and evaluation of different  
445 methods. *J. Hydrol.* 456, 12–29. doi:10.1016/j.jhydrol.2012.05.052
- 446 Themeßl, M.J., Gobiet, A., Heinrich, G., 2011. Empirical-statistical downscaling and error  
447 correction of regional climate models and its impact on the climate change signal.  
448 *Clim. Change* 112, 449–468. doi:10.1007/s10584-011-0224-4
- 449



## 450 **List of Figures**

451 Figure 1: The transfer function (heavy black line) between observed (bottom histograms)  
452 and modelled (histograms on the left) for the reference period (1981-2010) is used to  
453 adjust bias of a 30-year moving window starting from 1981-2010 to 2068-2097. The  
454 rightmost plot shows the residual histogram after bias correction. The change in the  
455 average correction (red mark) on the TF in comparison to the reference period mean  
456 correction (square) is shown.

457 Figure 2: a) Annual averages of temperature of the raw model data, the observations and  
458 the bias correction with and without the NSM, for the calibration period 1850 – 1899 (solid  
459 lines) and the validation period 1900-2005 (dashed). Probability densities of annual (c)  
460 and of daily means (d).

461 Figure 3: The EOBS and the RCM models' mean and standard deviation for the reference  
462 period 1951-2005. Differences (DIFF) indicate the [RCM statistic – EOBS statistic].

463 Figure 4: The 6-fold cross validation scheme with the calibration (C) and the validation  
464 (V) periods of each fold. Each experiment (Exp) was replicated for all five RCM models.

465 Figure 5: Mean surface temperature of the cross validation test.

466 Figure 6: Long-term linear trend [ $^{\circ}\text{C}/100 \text{ y}$ ] in the raw data (left) for the mean annual  
467 temperature (top) and the 10<sup>th</sup> and 90<sup>th</sup> (p10 and p90) percentiles the change in the trend  
468 relatively to the raw data trend is provided for the BC (middle) and the BC<sub>NSM</sub> data (right).  
469 All values are expressed as degrees per century.

470 Figure 7: Average of standard deviations for the study domain, for the raw data (a), the  
471 BC (b) and the BC<sub>NSM</sub> (c) for the different models and the observations, in annual basis.  
472 Differences between the raw and the bias corrected standard deviations are shown in (d)  
473 and (e). Plots (f) and (g) correspond to the same data as (d) and (e), but normalized for  
474 their 1951-2005 mean.

475

476



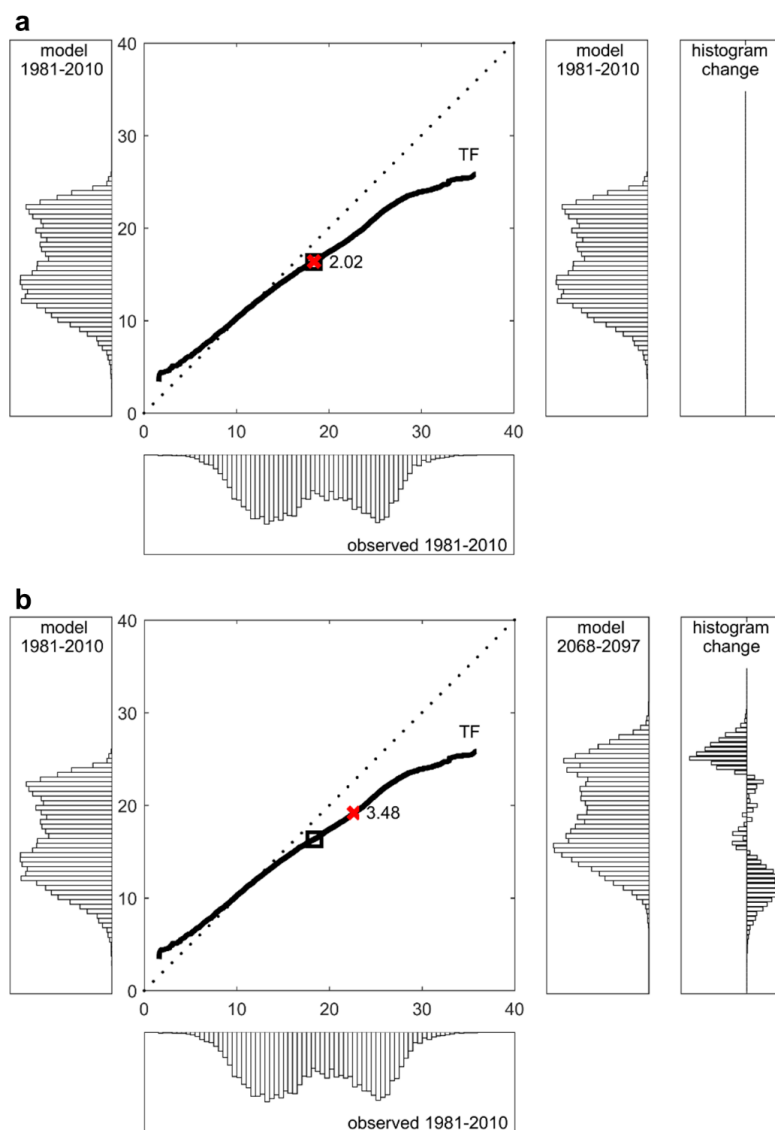
477 **List of Tables**

478 Table 1: Statistical properties of the calibration and the validation periods for the two bias  
479 correction procedures. Variables denoted with \* are estimated on annual aggregates. SD  
480 stands for standard deviation and pn for the nth quantile.

481 Table 2: RCM models used in this experiment.

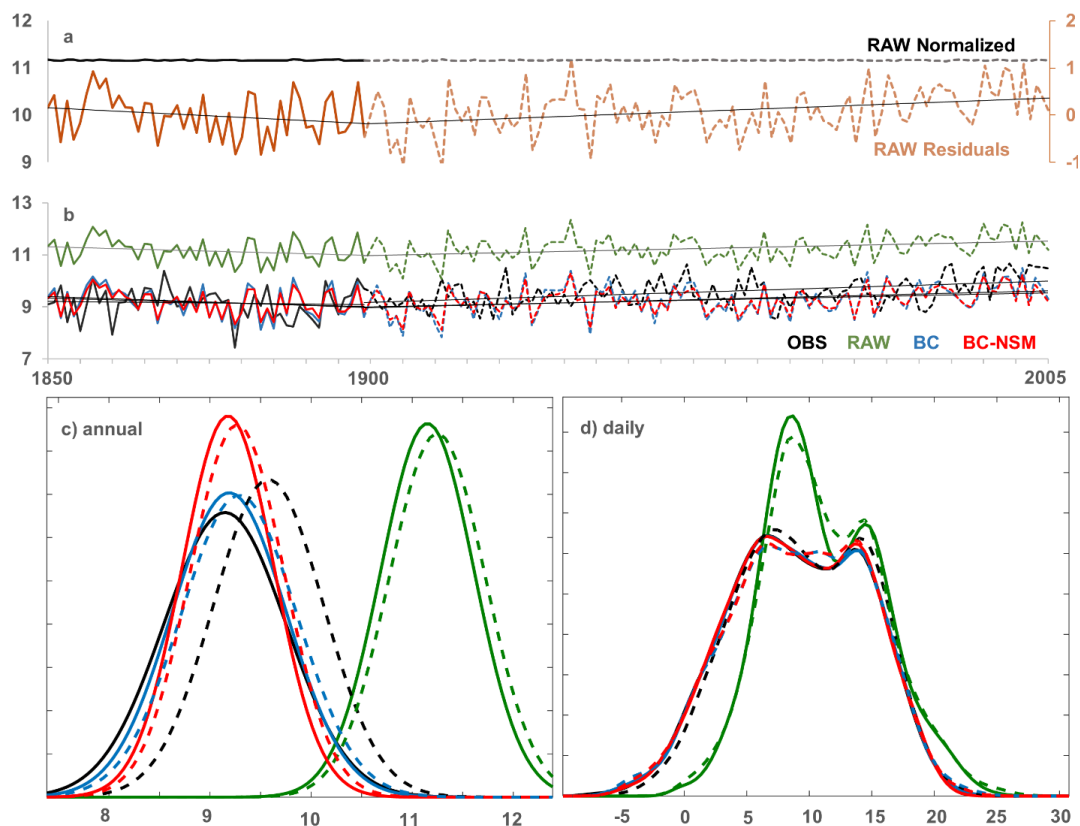
482

483



484

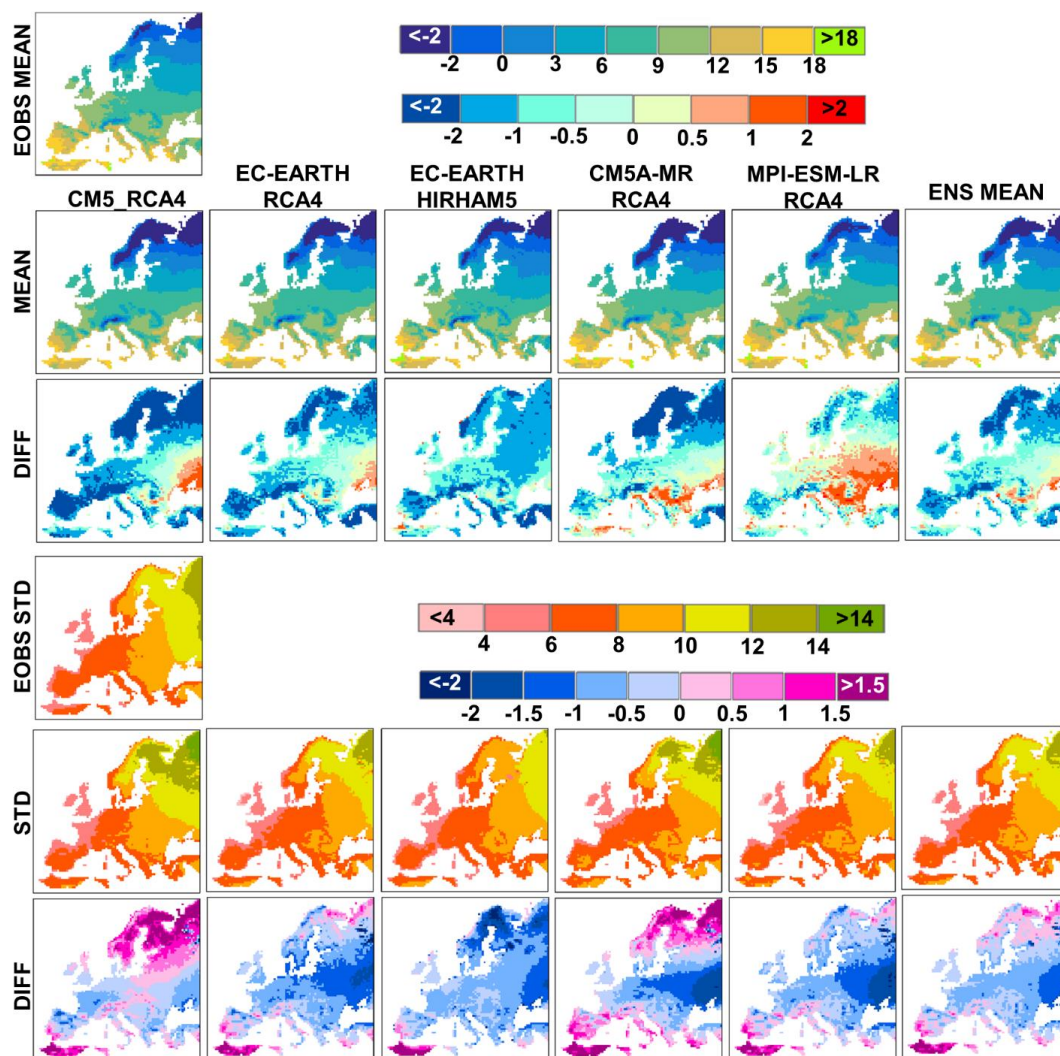
485 **Figure 1: The transfer function (heavy black line) between observed (bottom histograms) and**  
486 **modelled (histograms on the left) for the reference period (1981-2010) is used to adjust bias of a**  
487 **30-year moving window starting from 1981-2010 to 2068-2097. The rightmost plot shows the**  
488 **residual histogram after bias correction. The change in the average correction (red mark) on the**  
489 **TF in comparison to the reference period mean correction (square) is shown. The animated**  
490 **version provided in the supplemental material shows the temporal evolution of the bias as the 30-**  
491 **year time window moves on the projection data.**



492

493 **Figure 2: a) Annual averages of temperature of the raw model data, the observations and the bias**  
494 **correction with and without the NSM, for the calibration period 1850 – 1899 (solid lines) and the**  
495 **validation period 1900-2005 (dashed). Probability densities of annual (c) and of daily means (d).**

496



497

498 **Figure 3: The EOBS and the RCM models' mean and standard deviation for the reference period**  
 499 **1951-2005. Differences (DIFF) indicate the [RCM statistic – EOBS statistic].**

500

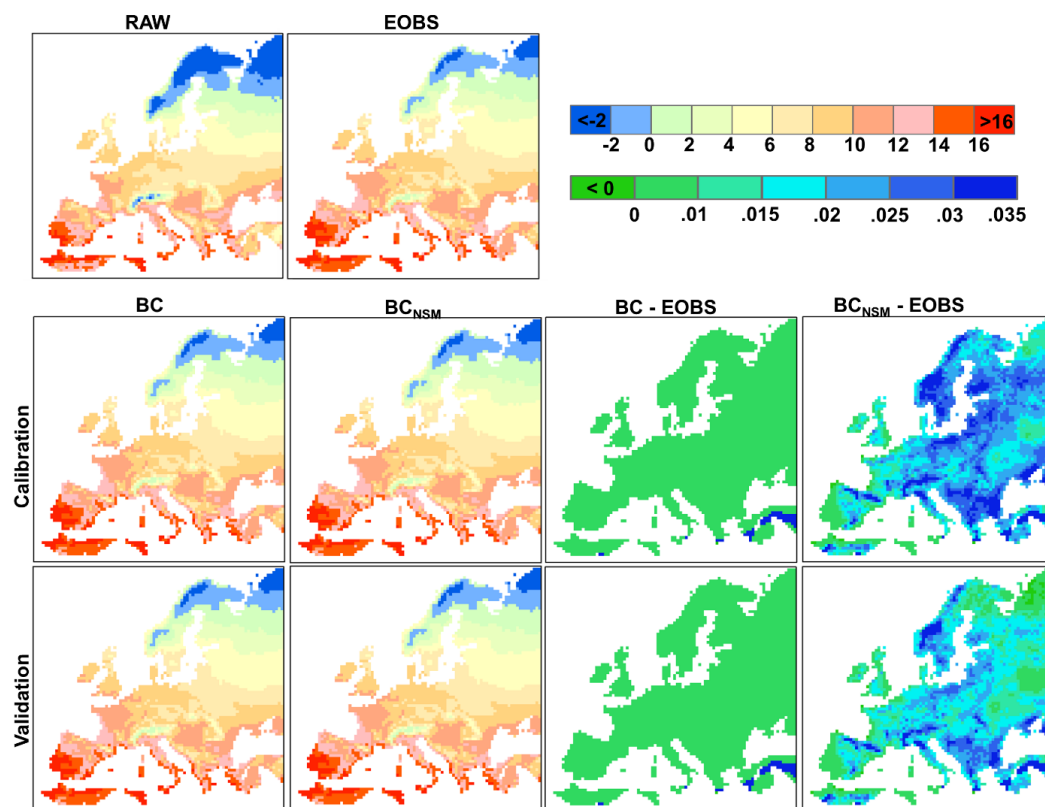


Fold	1	2	3	4	5	6
Exp 1	C	C	C	C	C	V
Exp 2	C	C	C	C	V	C
Exp 3	C	C	C	V	C	C
Exp 4	C	C	V	C	C	C
Exp 5	C	V	C	C	C	C
Exp 6	V	C	C	C	C	C
	1951-1960	1961-1970	1971-1980	1981-1990	1991-2000	2001-2010

501

502 **Figure 4: The 6-fold cross validation scheme with the calibration (C) and the validation (V) periods**  
503 **of each fold. Each experiment (Exp) was replicated for all five RCM models.**

504

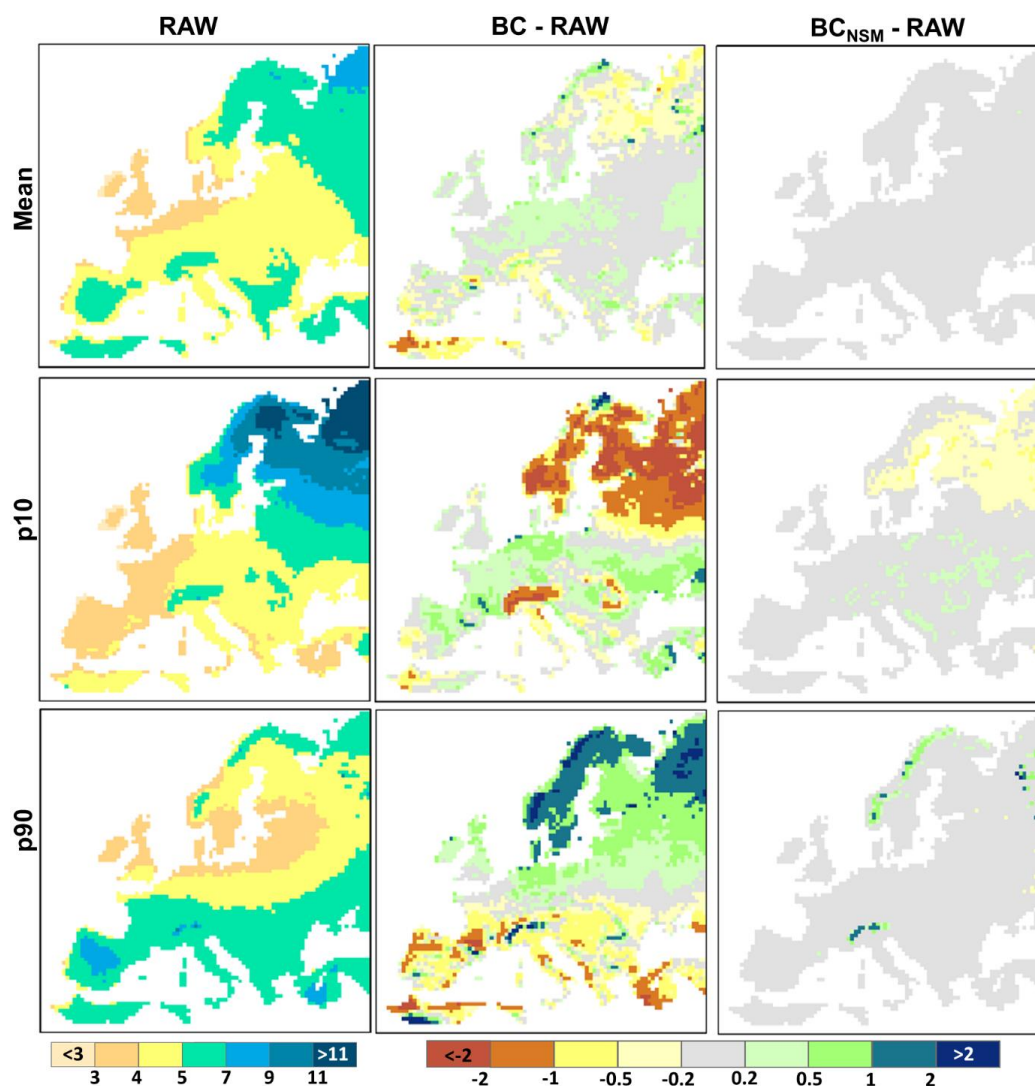


505

506

507

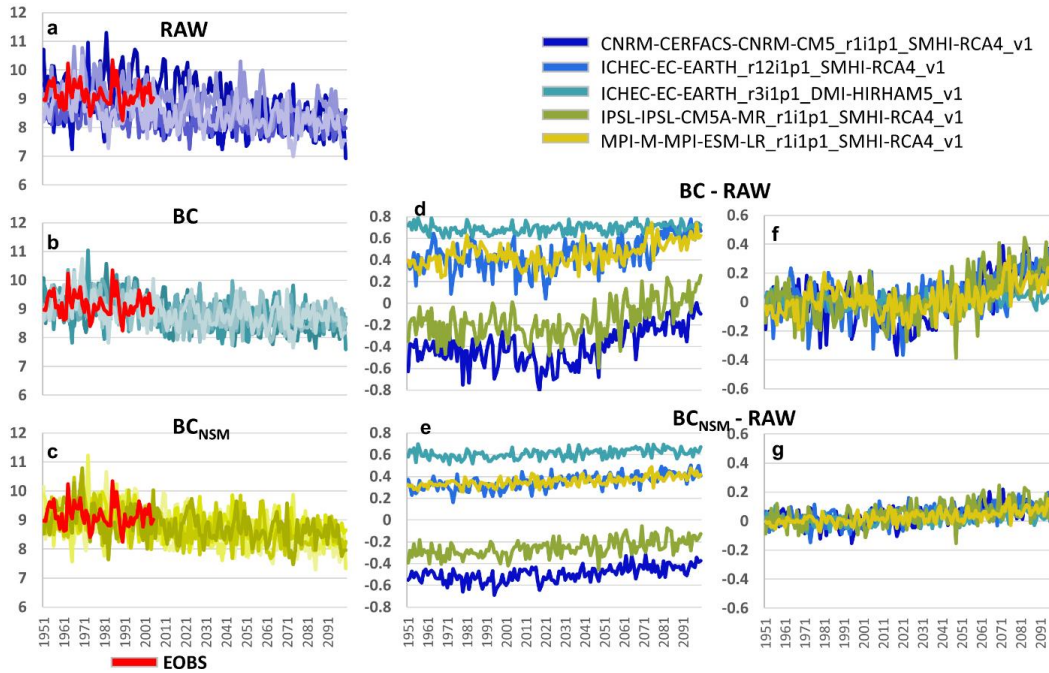
Figure 5: Mean surface temperature of the cross validation test.



508

509 **Figure 6: Long-term linear trend [ $^{\circ}\text{C}/100\text{ y}$ ] in the raw data (left) for the mean annual temperature**  
510 **(top) and the 10<sup>th</sup> and 90<sup>th</sup> (p10 and p90) percentiles the change in the trend relatively to the raw**  
511 **data trend is provided for the BC (middle) and the BC<sub>NSM</sub> data (right). All values are expressed as**  
512 **degrees per century.**

513



514

515 **Figure 7: Average of standard deviations for the study domain, for the raw data (a), the BC (b) and**  
 516 **the BC<sub>NSM</sub> (c) for the different models and the observations, in annual basis. Differences between**  
 517 **the raw and the bias corrected standard deviations are shown in (d) and (e). Plots (f) and (g)**  
 518 **correspond to the same data as (d) and (e), but normalized for their 1951-2005 mean.**

519

520



521 **Table 1: Statistical properties of the calibration and the validation periods for the two bias**  
 522 **correction procedures. Variables denoted with \* are estimated on annual aggregates. SD stands**  
 523 **for standard deviation and pn for the n<sup>th</sup> quantile.**

	Parameter	RAW	Normalized	Residuals	OBS	BC	BC <sub>NSM</sub>
Calibration	Slope [°C/10yr]*	-0.067	0.000	-0.067	-0.026	-0.086	-0.065
	Mean [°C]	11.2	11.2	0.0	9.1	9.2	9.2
	SD [°C]	4.5	4.6	0.9	5.3	5.3	5.3
	p5 [°C]	4.4	4.4	-1.4	0.4	0.5	0.5
	p95 [°C]	19.4	19.1	1.5	17.6	17.7	17.6
Validation	Slope [°C/10yr]*	0.052	0.000	0.051	0.076	0.062	0.051
	Mean [°C]	11.3	11.2	0.1	9.6	9.3	9.3
	SD [°C]	4.7	4.6	0.9	5.2	5.5	5.4
	p5 [°C]	4.2	4.4	-1.3	1.1	0.2	0.3
	p95 [°C]	19.4	19.1	1.5	17.6	17.7	17.6

524

525



526

**Table 2: RCM models used in this experiment.**

#	{GCM}_{realization}_{RCM}
1	CNRM-CM5_r1i1p1_SMHI-RCA4_v1
2	EC-EARTH_r12i1p1_SMHI-RCA4_v1
3	EC-EARTH_r3i1p1_DMI-
4	IPSL-CM5A-MR_r1i1p1_SMHI-
5	MPI-ESM-LR_r1i1p1_SMHI-

527